Viscous + Dahl model for MR dampers characterization:
A Real time hybrid test (RTHT) validation

N. Aguirre, F. Ikhouane & J. Rodellar
Department of Applied Mathematic III, Technical University of Catalunya, Spain.

D. J. Wagg & S. A. Neild
Department of engineering Mechanics.University of Bristol, UK.

ABSTRACT

Magnetorheological dampers have raised as promising devices for structural seismic protection since they have many attractive features such as small power requirements, reliability, and relatively low cost. These devices have strongly nonlinear behaviour which is very difficult to characterize. For this reason, the modelling of MR dampers has been an active field during the last years and has produced several models by combining a physical insight with a black-box approach. Among them, the so called "viscous + Dahl model" has been introduced as a particular case of the normalized version of the Bouc-Wen. Viscous + Dahl model is indeed significantly simpler than some other approaches and has well established conditions to ensure its physical and mathematical consistency.

This work deals with the modelling and identification of a small scale MR damper which is described by the viscous + Dahl model. The obtained model is validated experimentally into a real time hybrid test (RTHT) configuration where the MR damper is working as the seismic protection of a civil structure. The results show a good match between experimental and predicted forces.

Keywords: MR dampers, identification, Real time hybrid test, Dahl model.

1. INTRODUCTION

Magnetorheological dampers have raised as a promising devices for seismic protection since they have many attractive features such as small power requirements, reliability, and relatively low cost. These devices have a controllable fluid composed of suspensions of micron-sized, magnetizable particles dispersed in an appropriate carrier liquid. In the presence of a magnetic field the MR fluid becomes semisolid exhibiting a viscoplastic behaviour whose resistance depends on the magnitude of the applied magnetic field. Thus, through this transformation MR dampers can provide civil structural systems with adjustable additional damping which can be driven through an external input voltage.

The modelling of these devices from the laws of physics leads to models too complex to be used in control applications. For this reason, alternative models have been developed by combining a physical insight with a black-box approach (Savaresi et al. (2005)).

One of these models that has been used to describe MR dampers is the Dahl model (Dahl (1968)) which consists of a first-order nonlinear differential equations that approximates experimentally observed hysteresis loops. It has been used, among others, in references Zhou et al. (2006), Ikhouane and Rodellar (2007), Ikhouane and Dyke (2007) and Rodriguez et al. (2009) to describe the MR dampers behaviour.

The objective of this work is to model and identify a small scale MR damper described by a modified version of the Dahl model. Results are validated by a real time hybrid test (RTHT) where the MR damper is working as the seismic protection of a small scale civil structure. By doing this, the MR damper device is provided with realistic displacement and voltage signals, and thus a more appropriate validation of the model is obtained.

2. MODELLING AND IDENTIFICATION OF MR DAMPER

This section deals with the MR damper description using the viscous + Dahl model referred to in Ikhouane and Dyke (2007). This model has been derived as a match point of the normalized version of the Bouc-Wen model (Ikhouane and Rodellar (2007)) and the Bingham model (Spencer Jr et al. (1997)) used to characterize MR dampers behaviour.

The model is formulated as:

$$f(t) = \kappa_x[v(t)]\dot{x}_d(t) + \kappa_w[v(t)]w(t) \tag{2.1}$$

$$\dot{w}(t) = \rho[v(t)]\left(\dot{x}_d(t) - |\dot{x}_d(t)|w(t)\right) \tag{2.2}$$

where $\dot{x}_d(t)$ denotes the damper piston velocity, $v(t)$ the voltage input command, $f(t)$ is the damping force, w describes the nonlinear behaviour of the damper, and t refers to time. The viscous friction coefficient κ_x, the dry friction coefficient κ_w and the parameter ρ may be voltage dependent.

The identification methodology used in this paper is based on the results of Ikhouane and Rodellar (2007) and Ikhouane and Dyke (2007) where the input signal is chosen to be periodic as depicted in Fig. 2.1. In this case, the output force $f(t)$ of Eqn. 2.1 approaches asymptotically a periodic function $\overline{f}(t)$.
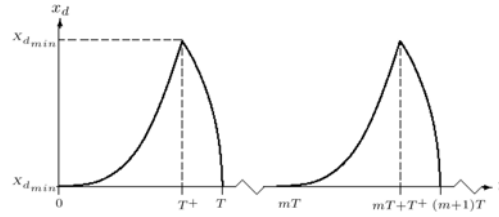

Figure 2.1. Input signal $x_d(t)$

The identification procedure assumes the knowledge of the hysteresis loop $\left(\overline{f}(\tau), x(\tau)\right)$ parameterized with the variable $\tau \in [0, T]$.

In that references it is shown that the hysteresis loop has a plastic region when the displacement is large enough. This region is characterized by $\overline{w}(\tau) \approx 1$. In this case, Eqn. 2.1 becomes

$$f(t) = \kappa_x[v(t)]\dot{x}_d(t) + \kappa_w[v(t)]. \tag{2.3}$$

This equation is linear in $\dot{x}_d(t)$ so that constants κ_x and κ_w can be determined by a linear regression.

Then, the parameter ρ is computed as:

$$\rho = \frac{a}{\kappa_w}. \tag{2.4}$$

Where constant a can be computed as explained in Aguirre et al. (2010).

Then, the identification results referred to in Aguirre et al. (2010), show that ρ is a voltage independent parameter so that it is taken as the mean value $\overline{\rho} = 47.95 \ (\text{cm}^{-1})$.

Parameters κ_x and κ_w are voltage dependent in the form

$$\kappa_x(v) = \kappa_{x_a} + \kappa_{x_b} v \tag{2.5}$$

$$\kappa_w(v) = \kappa_{w_a} + \kappa_{w_b} v \tag{2.6}$$

with $\kappa_{x_a} = 9.78\,(\mathrm{Ns\,cm^{-1}})$, $\kappa_{x_b} = 40.75\,(\mathrm{Ns\,cm^{-1}\,V^{-1}})$, $\kappa_{w_a} = 60.11\,(\mathrm{N})$ and $\kappa_{w_b} = 344.78\,(\mathrm{NV^{-1}})$ so that the MR damper model is obtained as:

$$f(t) = \left[\kappa_{x_a} + \kappa_{x_b} v(t)\right]\dot{x}_d(t) + \left[\kappa_{w_a} + \kappa_{w_b} v(t)\right]w(t) \tag{2.7}$$

$$\dot{w}(t) = \rho\left(\dot{x}_d(t) - \left|\dot{x}_d(t)\right|w(t)\right) \tag{2.8}$$

$$w(0) = \frac{f(0) - \left[\kappa_{x_a} + \kappa_{x_b} v(0)\right]\dot{x}_d(0)}{\kappa_{w_a} + \kappa_{w_b} v(0)} \tag{2.9}$$

Finally, it is important to point out that the MR damper inputs (displacement $x_d(t)$ and voltage $v(t)$) are strongly related to the structural system response which the MR damper is attached to.

With this in mind, next section is devoted to the description of a civil structure which is provided with a MR damper for seismic protection. By doing so, we are obtaining realistic data for the MR damper displacement and voltage inputs to be used in the validation of model 2.7 – 2.9.

3. SEMIACTIVE CONTROL OF A STRUCTURAL SYSTEM USING THE MR DAMPER

The structure under study is the 2-story building shown in Fig. 3.1 which is equipped with a MR damper between the ground (fixed base) and the first floor.
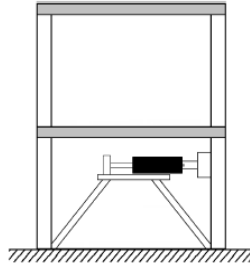

Figure 3.1. 2-story building equipped with a MR damper

Assuming that the structure is provided by a control force adequate to keep the response of the system in the linear region, equations of motion can be formulated as:

$$M\ddot{Q} + C\dot{Q} + KQ = -M\Gamma\ddot{x}_g + \Lambda f \tag{3.1}$$

where $Q = [x_1, x_2, ..., x_n]^T$, $\dot{Q} = [\dot{x}_1, \dot{x}_2, ..., \dot{x}_n]^T$ and $\ddot{Q} = [\ddot{x}_1, \ddot{x}_2, ..., \ddot{x}_n]^T$, correspond to the displacement, velocity and acceleration relative to the base, $\ddot{x}_g$ is the ground acceleration relative to an inertial reference frame and f corresponds to the MR damper force.

Matrices M, K and C represent the mass, stiffness and damping of the structure respectively.

$$M = \begin{bmatrix} 1.458 & 0 \\ 0 & 1.458 \end{bmatrix} \frac{\mathrm{Ns}^2}{\mathrm{cm}} \quad K = \begin{bmatrix} 1311 & -655.5 \\ -655.5 & 655.5 \end{bmatrix} \frac{\mathrm{N}}{\mathrm{cm}} \quad C = \begin{bmatrix} 2.489 & -0.830 \\ -0.830 & 1.659 \end{bmatrix} \frac{\mathrm{Ns}}{\mathrm{cm}}$$

Vector $\Gamma = [1,1]^T$ defines the influence of the external excitation $\ddot{x}_g$ over the entire structural system and matrix $\Lambda = [-1,0]^T$ sets the placement of the damper in the structure.

Eqn. 3.1 can be represented in the state space form as:

$$\dot{X} = A_s X + B_s f + E_s \ddot{x}_g \tag{3.2}$$

$$y = C_y X + D_y f \tag{3.3}$$

$$A_s = \begin{bmatrix} 0_{n\times n} & I_{n\times n} \\ -M^{-1}K & -M^{-1}C \end{bmatrix} \quad B_s = \begin{bmatrix} 0_{n\times 1} \\ M^{-1}\Lambda \end{bmatrix} \quad E_s = \begin{bmatrix} 0_{n\times 1} \\ -\Gamma \end{bmatrix}$$

$$C_y = \begin{bmatrix} -M^{-1}K & -M^{-1}C \end{bmatrix} \quad D_y = \begin{bmatrix} M^{-1}\Lambda \end{bmatrix}$$

where $X = [x_1, x_2, ..., x_n, \dot{x}_1, \dot{x}_2, ..., \dot{x}_n]^T$ is the state vector of the system and y is the regulated output vector (absolute accelerations of all floors). Variables $x_i, \dot{x}_i$ and $\ddot{x}_i$ are the displacement, velocity and acceleration of the floors respectively, all of them relative to the base.

It can be seen that in this case the MR damper displacement corresponds to the relative one of the first floor so that $x_d(t) = x_1$. The voltage signal $v(t)$ is computed from the "clipped optimal control" algorithm which is implemented with the objective of regulating the absolute accelerations of the structure. This strategy has been very often used in the literature for semiactive structural control applications as evidenced, among others, in Dyke et al. (1996), Yoshioka et al. (2002), Shook et al. (2007) and Johnson et al. (2007).

As a conclusion, Fig. 3.2 illustrates schematically the real application of the MR damper when working as the seismic protection of the structural system shown in Fig 3.1.
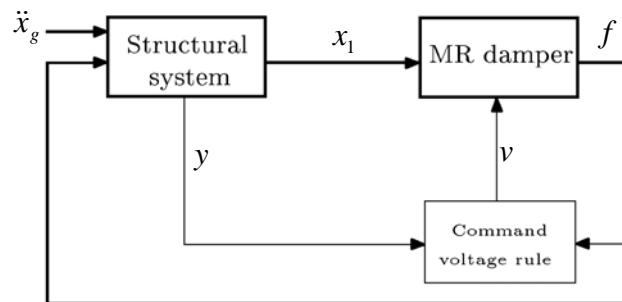

Figure 3.2. Semiactive control configuration

4 REAL TIME HYBRID TESTING (RTHT)

Real-time substructure testing is a method for establishing the dynamic behaviour of structural systems. The method separates a complex structure into physical and numerically modelled substructures, which interact in real-time allowing time-dependent nonlinear behaviour of the physical specimen to be accurately represented (Benzoni (2001), Sivaselvan et al. (2004)).

In our case, we need to describe the behaviour of the MR damper inside the system shown in Fig. 3.2. The experiment has been suited so that the numerical part simulates the structural system along with

the command voltage rule and the physical one corresponds to the MR damper which is the component we are interested in.

The experiment works by the exchange of information between the numerical and physical part as follows: The displacement of the first floor x_1 and the voltage signal v are computed from the numerical part and imposed via actuator device and voltage source on the MR damper. Then, the reaction force f generated by the MR damper is fed back to the numerical part to cycle again. This is illustrated in Fig. 4.1.
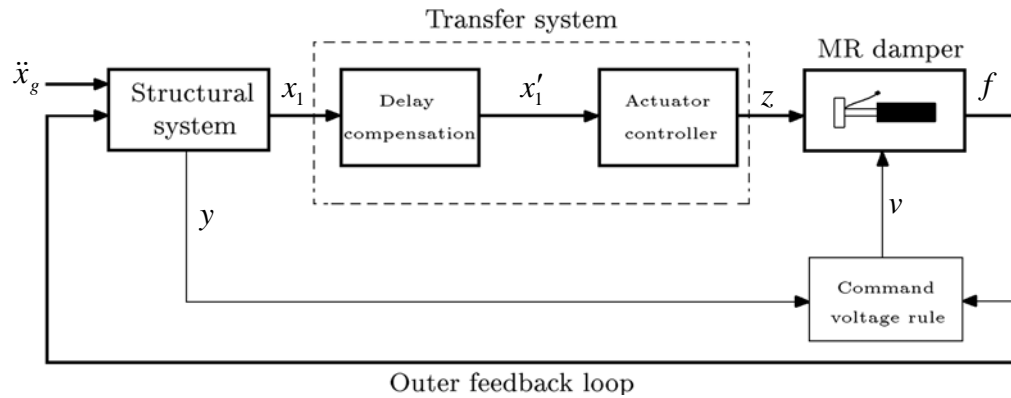

Figure 4.1. Configuration of the real time hybrid testing (RTHT)

The key feature of this testing method is the interaction between the numerical and physical components. Indeed, obtaining reliable results requires accurate compensation of the delayed response of the actuator, otherwise instability of the feedback loop is likely to occur (Carrion and Spencer (2006), Darby et al. (2002)).

To avoid this difficulty, a delay compensator is introduced into the transfer system as shown in Fig. 4.1. Then, signal x_1 is feed into the transfer system where the delayed compensated signal x'_1 is established as the set point for the controller so that the actuator output z tracks the demand signal x_1 as close as possible. Thus, the idea of the delay compensation is that once x'_1 get into the transfer system it will be delayed again to get $z = x_1$. In our case, the delayed compensated signal x'_1 is obtained by the forward prediction technique referred to in Wallace et al. (2005).

5. EXPERIMENTAL SETUP

Fig. 5.1 illustrates schematically how a real time hybrid test (RTHT) works. An electromechanical actuator commands displacement signals to the MR damper which at the same time is fed with a voltage signal from a voltage source which is driven by the command voltage rule. Then, the MR damper force is measured by a load cell and this signal is sent to the numerical part to compute the new displacement and voltage signals to cycle again.

Signals go from the numerical model to the physical one and the opposite by an acquisition system. The numerical components are written in the Matlab Simulink environment and run in real-time on a DSP using a dSpace DS1104 Controller Board. The experiment is conducted at the University of Bristol at BLADE laboratory using the experimental setup illustrated in Fig 5.2.

The transfer system is a linear electro-mechanical actuator attached to a centralizing plate which is free to run via linear bearings on two guide rails. The MR damper is the RD-1005-3 damper which is manufactured by Lord Corporation (http://www.lord.com/). It is 15.5 cm long, has an available stroke of 5.3 cm. It can generate damper forces (peak to peak) of > 2224N (0.05 ms^{-1} at 1 Amp) and $<$

667N (0.20 $\mathrm{m\,s}^{-1}$ at 0 Amp) and can operate till a temperature of 71ºC. The damper's accumulator can accommodate a temperature change in the fluid of 27ºC.
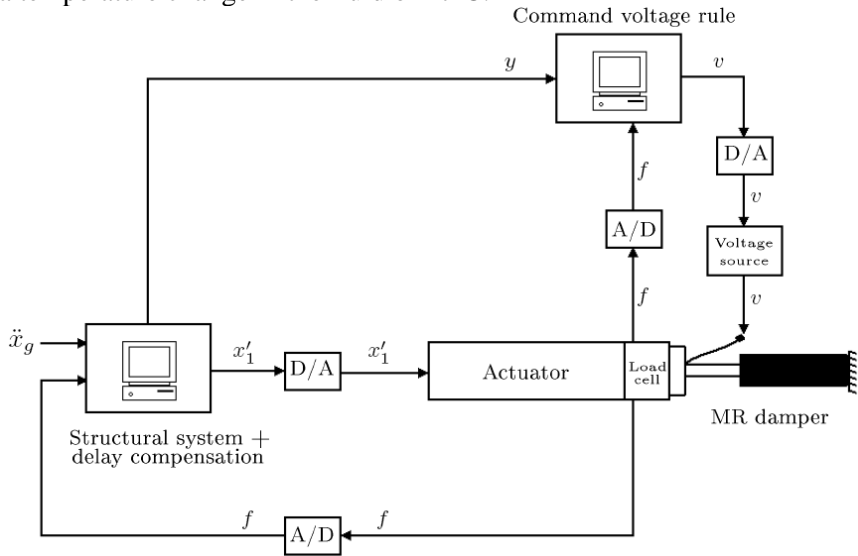

Figure 5.1. Experimental set-up scheme

(a)   (b)

Figure 5.2. Experimental set-up

6. EXPERIMENTAL RESULTS

To trigger the test indicated in Fig. 5.2, the structural system of Eqn. 3.1 is subject to an external excitation $\ddot{x}_g$ which corresponds to "El Centro" earthquake illustrated in Fig. 6.1 This excitation makes the MR damper to work due to the induced displacement and voltage inputs.
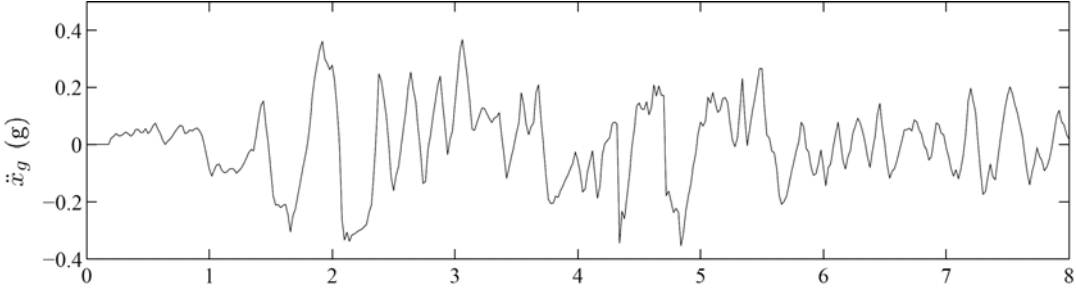

Figure 6.1. "El Centro" earthquake

Fig. 6.2.a illustrates the comparison between the desired MR damper displacement x_1 which comes from the numerical model of the structure (relative first floor displacement) and the actual position of

the MR damper z. it can be seen that the actuator delay has been successfully compensated since signals x_1 and z are in very good agreement. Fig. 6.2.b shows the corresponding synchronization plot which is not far from perfect synchronization which would yield a straight diagonal line.
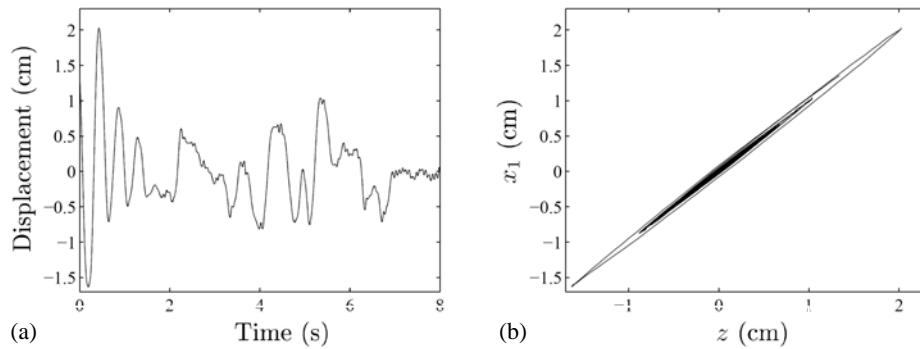

Figure 6.2. Compensation delay effectiveness. (a) Comparison between MR damper commanded displacement x_1 (solid line) and the measured one z (dashed line). (b) Synchronization plot.

Fig. 6.3 shows the MR damper displacement z, the voltage signal $v(t)$ computed from the semiactive controller and the comparison between the experimental and predicted force of the MR damper.

The discrepancy between the experimental and predicted force f_e and f respectively is measured by the L^1 norm as $\varepsilon = \dfrac{\|f_e - f\|_1}{\|f_e\|_1}$ where $\|g\|_1 = \int_0^{T_e} |g(t)| dt$. T_e and g are the time duration and force time function for each experiment.

In our case, force responses from Fig. 6.3.c yield an error of $\varepsilon = 20.2\%$ approximately which is acceptable for control applications.
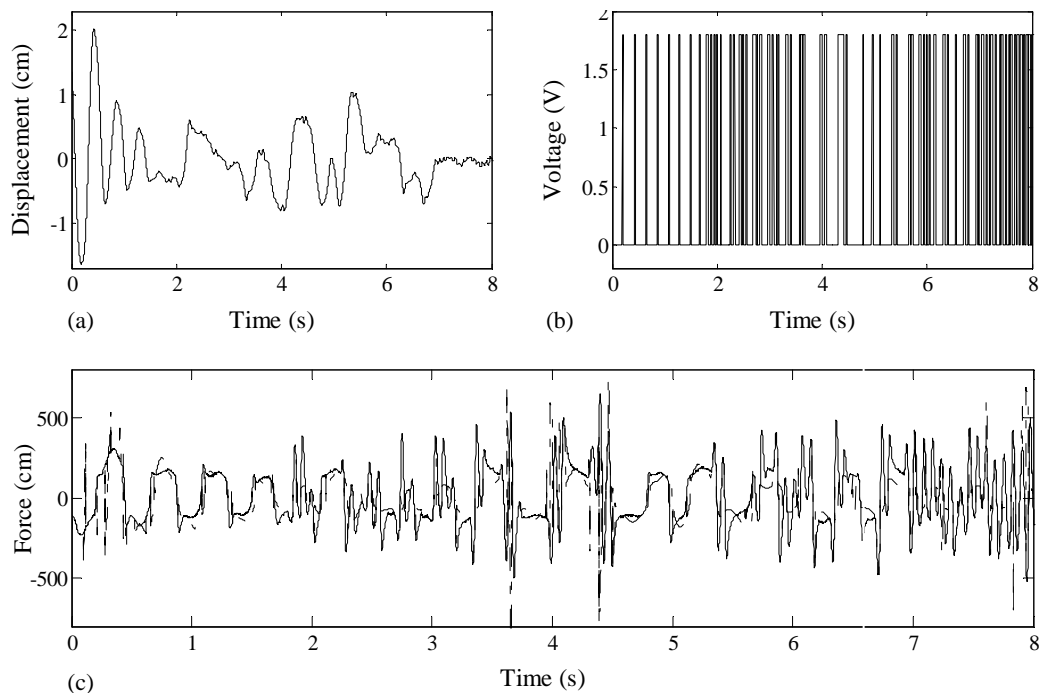

Figure 6.3. Real time hybrid test results. (a) MR damper displacement. (b) Input voltage. (c) Comparison between predicted force (dashed line) and experimental one (solid line).

7. CONCLUSION

This work has dealt with the modelling and identification of a small scale MR damper which is described by the viscous + Dahl model. Results are validated by a real time hybrid test (RTHT) of a small scale MR damper which is working as the seismic protection of a small scale civil structure. The results show good agreement between experimental force and the predicted one.

REFERENCES

Aguirre, N., Ikhouane, F., Rodellar, J. and Christenson, R. (2010). Modeling and identification of a small scale magnetorheological damper. *Proceedings of the IFAC International Workshop on adaptation and learning in control and signal processing*, Antalya, Turkey. (submitted).

Benzoni, G. (2001). Challenges of new generation seismic testing facilities. *Journal of Experimental Technique* **25:2**, 20-33.

Carrion, J. and Spencer, B. (2006). Real-time hybrid testing using model-based delay compensation. *Proceedings of the 4th International Conference on Earthquake Engineering* 299. Taipei, Taiwan.

Dahl, P.R. (1968). A solid friction model.*Technical Report* TOR-0158(3107-18)-1. The Aerospace Corporation, El Segundo, CA.

Darby, A.P., Williams, M.S. and Blakeboroug, A. (2002). Stability and delay compensation for real-time substructure testing. *ASCE Journal of Engineering Mechanics* **128:12**,1276-1284.

Dyke, S.J., Spencer Jr, B.F., Sain, M.K. and Carlson, J.D. (1996). Modeling and Control of magnetorheological dampers for seismic response reduction. *Journal of Smart Materials and Structures* **5**, 565-575.

Ikhouane, F. and Dyke, S. J. (2007) Modeling and identification of a shear mode magnetorheological damper. *Journal of Smart Materials and Structures* **16**, 605-616.

Ikhouane, F. and Rodellar, J. (2007). Systems with Hysteresis: Analysis, Identification and Control Using the Bouc-Wen Model. (Chichester, UK: Wiley).

Johnson, E. A., Baker, G.A., Spencer Jr, B.F., and Fujino, Y. (2007). Semiactive damping of stay cables. *Journal of Engineering Mechanics* **133:1**, 1-11.

Rodriguez, A., Ikhouane, F., Rodellar, J. and Luo, N. (2009). Modelling and identification of a small-scale magnetorheological damper. *Journal of Intelligent Material Systems and Structures* **20:7**, 825-835.

Savaresi, S.M., Bittanti, S. and Montiglio, M. (2005). Identification of semi-physical and blackbox non-linear models: The case of MR dampers for vehicles control. *Automatica* **41:1**, 113-127.

Sivaselvan, M.V., Reinhorn, A., Liang, Z. and Shao, X. (2004). Real-time dynamic hybrid testing of structural systems. *Proceedings of the 13th Earthquake Engineering Conference* 1644. Vancouver, B.C., Canada.

Shook D., Lin, P.Y., Lin, T.K. and Roschke P**. N.** (2007)**.** A comparative study in the semi-active control of isolated structures. *Journal of Smart Materials and Structures* **16**, 1433-1446.

Spencer Jr, B.F., Dyke, S.J., Sain, M. K. and Carlson, J.D. (1997). Phenomenological model for a magnetorheological damper. *ASCE Journal of Engineering Mechanics* **123:3**, 230-238.

Wallace, M., Wagg, D. and Neild, S. (2005). An adaptive polynomial based forward prediction algorithm for multi-actuator real-time dynamic substructuring. In Proceedings of the Royal Society Series A **461**, 3807-3826.

Yoshioka, H., Ramallo, J.C. and Spencer Jr, B.F. (2002) "Smart" Base Isolation Strategies Employing Magnetorheological Dampers. *Journal of Engineering Mechanics* **128:5**, 540-551.

Zhou, Q., Nielsen, S.R.K. and Qu, W.L. (2006). Semi-active control of three-dimensional vibrations of an inclined sag cable with magnetorheological dampers. *Journal of Sound and Vibration* **296**, 1-22.